A numerical simulation of CPT test based on a cavity expansion theory by using effective stress analysis

T. Kawai / primary author
Tohoku University, Sendai, Japan, tadashi.kawai.b2@tohoku.ac.jp

T. Noda
Nagoya University, Nagoya, Japan, noda@civil.nagoya-u.ac.jp

K. Jimba
NEXCO East(Former graduate student of Tohoku University), Misato, Japan

ABSTRACT: Although the penetration resistance is not a physical parameter inherent to the soil material but is a value reflecting the response from the ground, there are many estimations that directly associate penetration resistance with various ground physical properties. Penetration resistance is subject to both the influence of the properties of the ground material such as strength parameters or dilatancy of the soil, and the influence of the boundary condition such as layer boundary and drainage condition around the target ground. Therefore, in order to improve the accuracy of the CPT, it is important to analyze the behavior of the soil by considering cone penetration as a complicated boundary value problem and clarify the influence of boundary conditions and soil characteristics on penetration resistance. In this study, a series of model penetration tests and their simulations was conducted in order to verify the adaptabilities of a cavity expansion theory by using effective stress analysis.

Keywords: FEM; effective stress analysis; penetration; model test; cavity expansion

1. Introduction

The Cone Penetration Test (CPT) is extensively used as an in-situ soil investigation method. The estimation of soil parameters, such as the internal friction angle, are typically performed using the cone penetration resistance obtained from the CPT. However, since cone penetration resistance is not a physical parameter unique to soil material but rather a response value of the ground, it is reasonable to assume that estimating soil parameters directly from cone penetration resistance is problematic, at best. Even though the cone penetration test is a proven method for evaluating soil properties, relatively little research has been conducted to understand penetrometer readings as a complicated boundary value problem.

One of the complicating factors in the interpretation of CPT data is that readings are influenced not only by the soil at the location of the cone tip but also by the soil within an influence zone which extends some distance both beneath and above the tip. Ahmadi & Robertson [1] studied the 'thin-layer effects' on the CPT-data. They conducted a series of FEM numerical analyses using so-called cavity expansion modeling and concluded that the full tip resistance may not be reached in thin stiff layers because of the influence of the upper/lower softer layers. Recently, Mo et al. [2] also conducted the similar systematic analysis and compared their numerical results with field data. Further, Mo et al. [2] conducted an extensive parametric study using large deformation finite-element analyses, then, based on their numerical results, they proposed a procedure for interpreting the layer boundaries and undrained shear strength from measured CPT-data after taking the thin-layer effect into account. Meanwhile, an experimental investigation by Mo et al. [3] obtained the extent of soil deformation around a penetrated cone using centrifuge testing. Their results revealed that the cone penetration is a complicated boundary value problem. As for the field CPT-data, Thevanayagam et al. [4] evaluated the relationships between liquefaction resistance and CPT-data and considered the combined effect of penetration velocity and the coefficient of consolidation Cv, which is composed of permeability k and compressibility mv. This can be considered field evidence that the cone penetration is a complicated boundary value problem. Therefore, in order to obtain the soil properties of the target location, the response behavior of the soil should be evaluated as a boundary value problem which takes the many factors shown in Fig. 1 into account at the same time: consolidation (drainage), shear deformation and the dilatancy of the target soil and its neighbor layers.

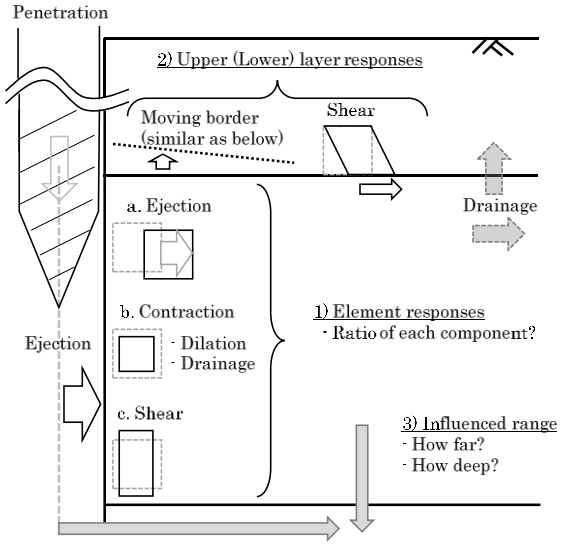

Figure 1. Penetration mechanisms; the logic solving it as a boundary value problem.

As preparation for a future numerical investigation focused on the details of the combined effects of soil properties and various boundary conditions, a series of numerical analyses was conducted using a FEM code named GEOASIA (All Soils All States All Round Geoanalysis Integration) developed by Asaoka et al. in [5, 6] and sophisticated by Noda et al. in [7], in which the Super/subloading Yield Surface Cam-clay model, in short, the SYS Cam-clay model in [8-10] was used as the constitutive equation of the soil skeleton. As shown in the results reported by Tolooiyan & Gavin in [11] from a series of numerical simulations using multiple soil modeling methods and obtaining different results, the soil modeling methods greatly influence the obtained results. As such, in order to evaluate the complicated boundary value problem, it is clearly necessary to adopt a more sophisticated model which represents soil behavior as close to reality as possible.

Among the various analysis methods of cone resistance, Mo et al. [2] adopted the so-called cavity expansion modeling to realize the soil responses during cone penetration after careful consideration of the experimental results. The validity of the modeling method was also carefully confirmed by Ahmadi et al. in [12] and Ahmadi & Dariani in [13]. Therefore, the same modeling method was adopted in this study. A description of the calculation procedures is firstly provided with some preliminary calculation results achieved by the use of various displacement ratios at the supposed cone apex and the upper rod.

There has been relatively little research done on the effect of soil dilatancy on CPT measurements related to layered configurations. Kawai et. al. [14] conducted a series of numerical simulations about this topic by using a sophisticated effective stress analysis code. Although the influences of the vertical displacement ratio at the cone apex or the shaft on the tip resistance were precisely investigated, influences of some basic conditions like FEM mesh size were not evaluated. Therefore, in this paper, the influence of mesh size on the tip resistance is confirmed at first. Then, as a part of preparations for future experimental validations through numerical simulations of a series of calibration chamber tests, a series of numerical parametric simulations evaluating the influence of lateral boundary conditions and confining pressure on cone tip resistances are conducted.

2. Numerical analysis - Models and settings

The finite element mesh and boundary conditions used are shown in Fig. 2. The over burden pressure, equivalent to the depth of 7.8 m with the same density as the soil, is given at the top of the model in order to avoid expected instabilities caused by very low confining pressure of the soil. For the same reason, a few nodes of the left border from the top, actually center of the axisymmetric model, are set free to move more leftward than the cone radius and a few nodes of the top of the model from the center are also set free to move more downward than the other top nodes. The effect of the gravity force was taken into account in the calculations. The penetration part is magnified in Fig. 3, the actual number of nodes to express the cone apex-part depends on the mesh size. As shown in Fig. 3, the nodal points on the left-hand side border of the FEM mesh, which were pushed away toward the right-hand side and downward along the supposed cone path, were directly moved to realize the ground movements during cone penetration by following the cavity expansion modeling described in [1] in detail. The nodal points were moved from the top one. The supposed cone apex angle and diameter were 60 degrees and 16 mm respectively modeling a miniature cone for a chamber test, then the horizontal displacement of each nodal point was as much as 8 mm after all calculation stages to reach the shaft radius; each calculation stage involved about 6000 time integration steps (time span 0.00005 s) at a cone penetration speed of about 5 mm/s toward the depth. These size and speed parameters were set as a preliminary study for future experimental validations by using a calibration chamber and a miniature cone.

The required material constants and the meaning of each parameter are listed in Table 1. The parameter values set for a model used in this study are given in Table 2 along with the initial values (Table 3) describing the initial soil state. These values are expected to provide a loose sand. Fig. 4 shows the element behavior (drained triaxial loading) using the SYS Cam-clay model with the triaxial shear test results obtained by using a fine silica sand at a relative density of 50 %.

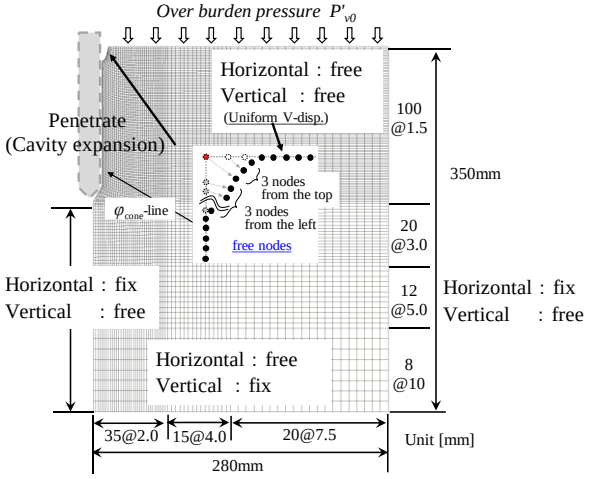

(a) Standard model (Mesh A)

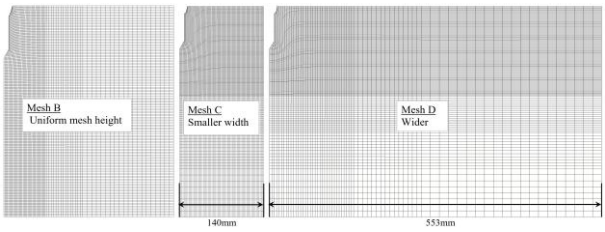

(b) Other models

Figure 2. Axisymmetric FEM mesh and boundary conditions.

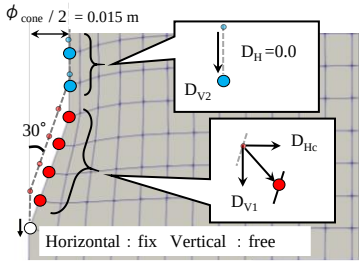

Figure 3. Calculated procedures of cone penetration.

Table 1. Meanings of each material property in SYS Cam-clay model

A. Elasto-plastic parameters	
A1	Compression index $\tilde{\lambda}$
A2	Swelling index $\tilde{\kappa}$
A3	Critical state constant M
A4	Specific volume at q=0 and p'=98.1 (kPa) on NCL N
A5	Poisson's ratio ν
B. Evolution rule parameters	
B1	Degradation index of structure a (b=c=1.0)
B2	Degradation index of overconsolidation m
B3	Evolution index of rotatioal hardening b_r
B4	Limit of rotational hardening m_b
C. Permeability k (cm/s)	
D. Specific gravity of soil particles Gs	

Table 2. Settings of the material parameters

A1: $\tilde{\lambda}$	A2: $\tilde{\kappa}$	A3: M	A4: N	A5: ν
0.06	0.001	1.2	1.75	0.2
B1: a	B2: m	B3: b_r	B4: m_b	
0.001	0.05	0.7	1	
C	0.0001	cm/s	D	2.66

Table 3. Settings of the initial conditions

Degree of structure $1/R^*$	3.0
Lateral stress ratio K_0	0.2
Specific volume v_0	1.6936

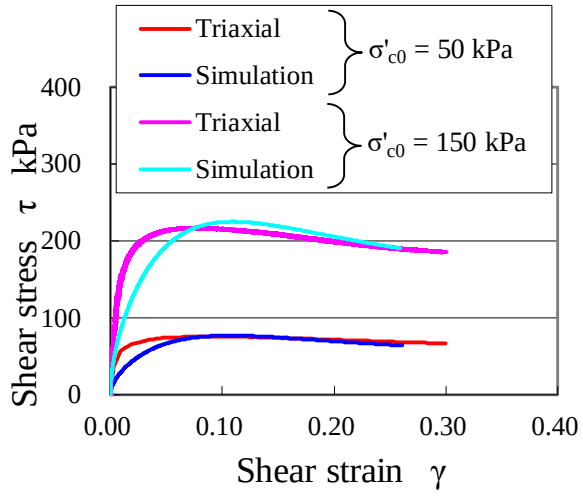

Figure 4. Examples of the element responses of SYS Cam clay model by using the material properties shown in Tables 2 and 3.

3. Results

Since the functions to define friction are limited at the border, i.e. FEM mesh boundary or the contact surface between two different materials, they are not implemented in the FEM code used in this study, and the magnitudes of the vertical displacements at the cone apex and rod must be prescribed. As the numerically achieved results of [1] and also the experimentally achieved results of [14] show, since the ratio of vertical displacement to horizontal displacement is dependent on the various conditions, e.g. material kinds, penetration speed and so on, there is no hint to determine the value of the ratio without a concrete target image. In abandoning any attempt to validate the value adopted in this study, Kawai et al. in [15] conducted a parametric study about the ratio of the vertical displacement to the horizontal one at the cone apex and concluded that it has a large influence on the tip resistance. As the ratio becomes larger, the tip resistance also increases. Since the main purpose of this paper is only comparisons of the numerical analysis results, a fixed value of 0.4 was set to the ratio for every numerical analysis case. All the cases conducted in this paper are listed in Table 4.

Table 4. Simulation cases

Case #	Mesh type	Over burden pressure P'v0 kPa
Case 1	A	68
Case 2	B	68
Case 3	C	68
Case 4	D	68
Case 5	A	43
Case 6	A	32
Case 7	A	18

3.1. Influence of FEM mesh size

Firstly, in order to obtain the basic performance of the cavity expansion method, the influence of mesh size was investigated. As shown in Fig. 2, several different mesh heights are adopted in the mesh A, C and D. On the other hand, the mesh B, which has a uniform element height, was also prepared to consider mesh size effects by comparing Case 1 and Case 2.

As shown in Fig. 5 and 6, the results from Case 1 and Case 2 are similar to each other not only in the tip resistance but also in the stress distributions. On the other hand, the tip resistance of Case 1 at the height of around -0.17 m shows a sudden change of the tendency and the height was at the location of the settled border of two different mesh heights. However, as shown in Fig. 6, because the volume of soil model was laterally enclosed by fixing the horizontal movements of the nodes on the lateral boundary during penetration, all the lateral stress increments were increased especially in the later stages of penetration and it might affect the sudden change of the tip resistance in Case 1.

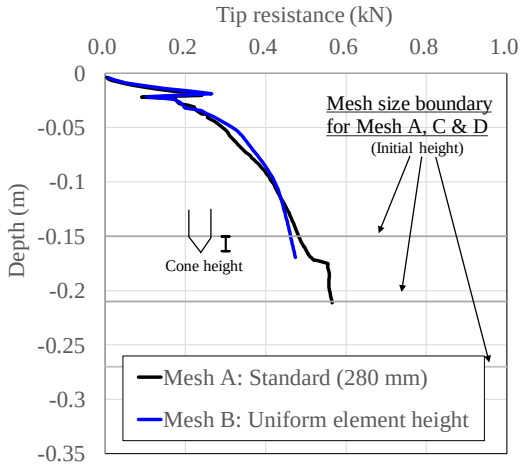

Figure 5. Confirmations of the extent of influence of element size at the cone apex on the tip resistance.

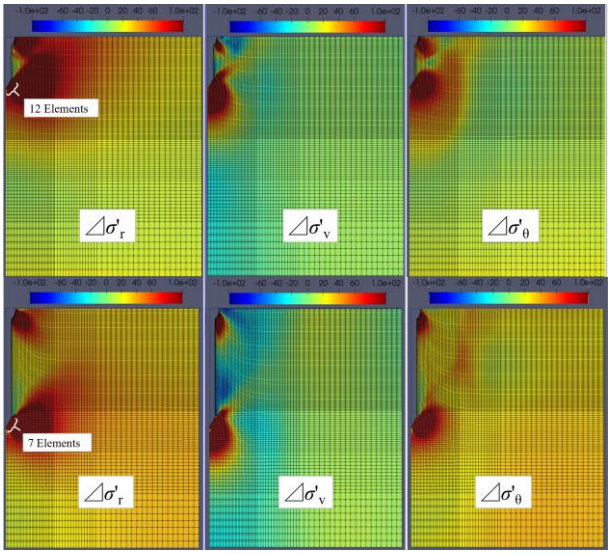

(a) Case 1

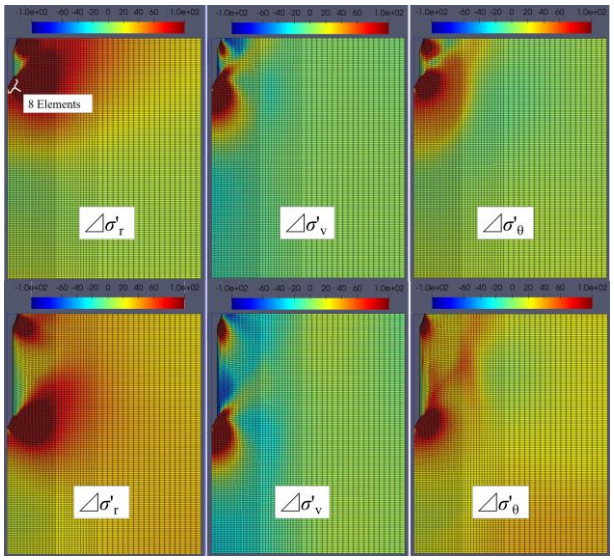

(b) Case 2

Figure 6. Confirmations of the extent of influence of element size at the cone apex on the stress increment distributions (kPa).

In order to confirm the extent of influence of the enclosed volume, the different lateral model size meshes, which are Mesh C and Mesh D in Fig. 2, were used for Case 3 and Case 4. The results are shown in Fig. 7 and 8.

As shown in Fig. 7, despite the difference of the model width and the resultant tip resistances in the range of -0.05 m to -0.17 m, the tip resistances of all the cases are close to each other. Further, it was observed that even in Case 4 using the wider model, there is a small disturbance at the point close to the border of the element height. Therefore, a small influence of the number of the elements to express the cone apex on the tip resistance seems to exist. In these simulations, since the material parameters were set to model a loose sand of the relative density of 50 %, even in the range of -0.05 m to -0.17 m, the gap of tip resistances between Case 3 (smaller width) and Case 4 (wider model) was not so large.

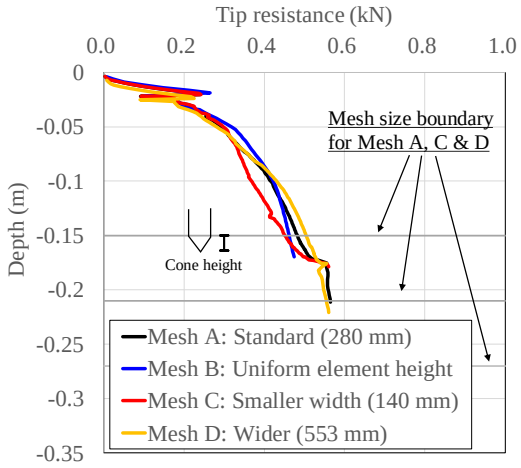

Figure 7. Confirmations of the extent of influence of element size at the cone apex on the tip resistance with using models having different width.

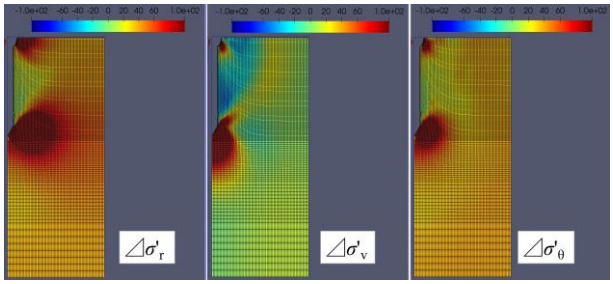

(a) Case 3: smalle width (140 mm)

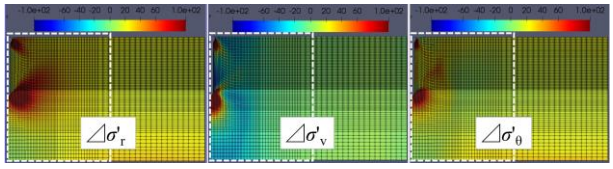

(b) Case 4: wider model (553 mm)

Figure 8. The stress increment distributions for Case 3 and Case 4.

3.2. Confirmations of dependency of penetration resistance on the confining pressure

Because there is no comparable result from a calibration chamber test so far, in order to evaluate the magnitude of the differences caused by the mesh size effect, a series of numerical simulations, shown in Table 4 as Case 5, 6 and 7, were conducted. This series was designated to

investigate the relationships between the initial over burden pressure and the tip resistance. In general, different depth leads to a different tip resistance for the same material, and the deeper the location is, the larger the tip resistance becomes. If the tendency can be easily recognizable in the range of a practical overburden pressure, it is proved that the mesh size effect can be negligible.

In Fig. 9, the results from Case 5, 6 and 7 are shown with the results from Case 1 and 2, in which the different meshes were used for the calculations under the same analytical conditions. As shown in Fig. 9, it was clearly observed that there is a relationship between the initial overburden pressure and the tip resistance. This demonstrates that parametric studies to investigate the influences of various soil conditions can be conducted using the cavity expansion method for the penetration phenomenon.

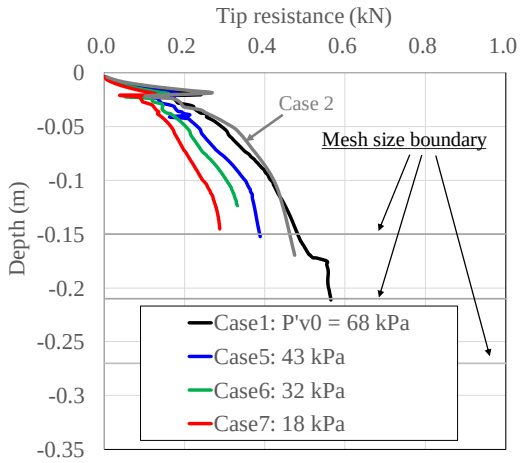

Figure 9. Confirmations of the realization of the relationships between the overburden pressure and the tip resistance.

3.3. Rough comparisons of penetration resistance from the numerical simulation with a calibration chamber test result

3.3.1. Outlines of a calibration chamber test

As a preliminary test, a few cases of calibration chamber tests were conducted by using a rigid box with a center whole and a pressure system at the surface of the ground by using a water pressure bag. Because of some unresolved difficulties with conducting well controlled tests, especially regarding the application of a homgeneous surface pressure using the water bag system, the results from these tests can be used only for a rough comparisons with the numerical results. The axisymmetric numerical model has the same volume as the experimental square box. The outlines of the model chamber test are shown in Fig. 10 and a typical result of earth pressure measurement is shown in Fig. 11. The measured results of earth pressure at the same height are rather scattered in Fig. 11. It is noted that the earth pressure recorded directly beneath the cone started to decrease, which means a reduction of the vertical stress despite penetration of the cone toward the earth pressure meter.

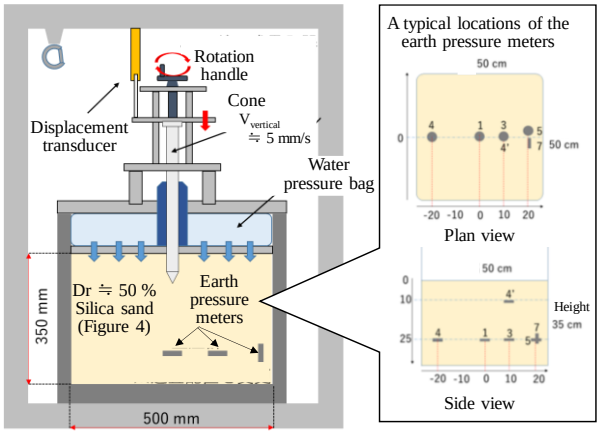

Figure 10. Outlines of a preliminary calibration chamber test.

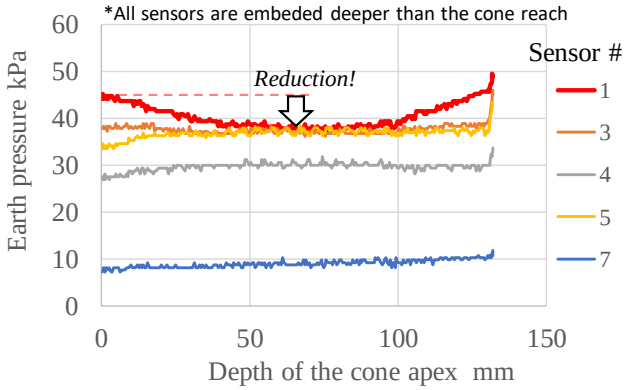

Figure 11. A typical measurement result of earth pressures.

3.3.2. Penetration resistances

In Fig. 12, all the experimental results are shown with the results from numerical simulations shown in Fig. 9. As shown in this figure, the simulated results are relatively smaller and located within a narrower range than those of the experimental results despite the larger range of the overburden pressure. However, as mentioned above, these experimental results are less reliable and the lack of information of the displacement ratio at the apex of the cone causes difficulties of realizing the tip resistance quantitatively. Therefore, although further investigations are needed, the results indicate at least that there is the possibility to reproduce cone penetrations by means of the cavity expansion method as also shown by the experimental results.

4. Summary

As preparation for a future numerical investigation on the details of the combined effects of soil properties and various boundary conditions on cone penetration resistance, a series of numerical analysis was conducted using a FEM code named GEOASIA. As a result, it is obtained that the number of elements to model a cone apex should be at least more than seven to make the difference caused by mesh size within a negligible range. This is confirmed by reproducing both the stress dependency of the tip resistances and the preliminary calibration chamber tests.

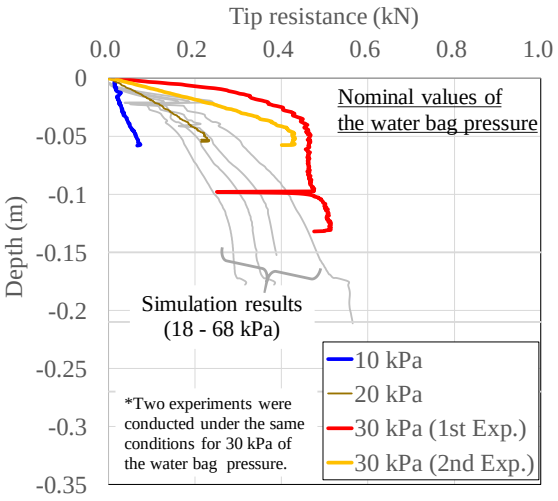

Figure 12. Comparisons of all the results obtained from both experiment and numerical simulations conducted at different over burden pressures.

References

[1] Ahmadi, M. M. & Robertson, P. K. "Thin-layer effects on the CPT qc measurement", Canadian Geotech. J. , 42(5) , pp. 1302-1317, 2005..

[2] Mo, P.Q., Marshall, A.M. & Yu, H.S. "Interpretation of cone penetration test data in layered soils using cavity expansion analysis", J. Geotech. Geoenviron. Eng., 143(1), pp. 04016084-1-12, 2017.

[3] Mo, P.Q., Marshall, A.M. & Yu, H.S. "Centrifuge modelling of cone penetration tests in layered soils", Geotechnique, 65(6), pp. 468-481, 2015.

[4] Thevanayagam, Sl, Sivaratnarajah, U. & Huang, Q. "Soil liquefaction screening using CPT - Effect of non-plastic silt content", Int. Symp, PBDIII, Paper #481, 2017.

[5] Asaoka A., Noda, T. & Kaneda, K. "Displace-ment/traction boundary conditions represented by constraint conditions on velocity field of soil", Soils and Foundations, 38(4) , pp. 173-181, 1998.

[6] Asaoka A. & Noda, T. "All soils all states all round geo-analysis integration, International Workshop on Constitutive Modelling – Development", Implementation, Evaluation, and Application, Hong Kong, China, pp. 11-27, 2007.

[7] Noda, T., Asaoka, A. & Nakano, M. "Soil-water coupled finite deformation analysis based on a rate-type equation of motion incorporating the SYS Cam-clay model", Soils and Foundations, 48(6) , pp.771-790, 2008.

[8] Asaoka, A., Nakano, M. & Noda, T. "Super loading yield surface concept for the saturated structured soils", Proc. 4th Eur. Conf. Num. Meth. Geotech. Engrg. NUMGE98, pp. 232-242, 1998.

[9] Asaoka, A., Nakano, M. & Noda, T. Superloading yield surface concept for highly structured soil behavior, Soils and Foundations, 40(2) , pp. 99-110, 2000.

[10] Asaoka, A., Noda, T., Yamada, E., Kaneda, K. & Nakano, M. "An elasto-plastic description of two distinct volume change mechanisms of soils", Soils and Foundations, 42(5) , pp. 47-57, 2002.

[11] Tolooiyan, A. & Gavin, K. Modelling the cone penetration test in sand using cavity expansion and arbitrary lagrangian eulerian finite element methods, Computers and Geotechnics, 38(4) , pp. 482-490, 2011.

[12] Ahmadi, M. M., Byrne, P. M. & Campanella, R. G. "Cone tip resistance in sand: modeling, verification, and applications", Canadian Geotech. J. , 42(4) , pp. 977-993, 2005.

[13] Ahmadi, M.M. & Dariani Golestani, A.A. "Cone penetration test in sand: A numerical-analytical approach", Computers and Geotechnics, 90 , pp. 176-189, 2017.

[14] Arshad, M.I., Tehrani, F.S., Prezzi, M. & Salgad, R., 2014. Experimental study of cone penetration in silica sand using digital image correlation, Geotechnique, 64(7), pp. 551-569.

[15] Kawai, T., Kubota, K., Kim, J. K., Kazama, M. and Noda, T. " Things measured by cone penetration tests other than material properties ", Proc. of the 1st Int. Conf. on Press-in Engineering, Kochi, pp. 401-408, 2018.